Report on SSA

Elisabeth Strøm[1]
AST4310 25.09.2017

[1] Institute of Theoretical Astrophysics, University of Oslo

Abstract. By using the Saha and Boltzmann law we are able to reproduce Cecilia Payne's work on the strength of spectral lines. We used the element schadeenium (E) to reproduce Schadee's tables. By using the Boltzmann distribution, we find that excitation never depletes the ground stage of an ion or atom, and that as the temperature increase, more levels s get a notable population density. For the Saha distribution only two ionization levels have a notable population density at each of the temperatures $T = 5\,000,\ 10\,000,\ 20\,000$ K. This is due to the Boltzmann factor dominating the other stages. The Saha-Boltzmann distribution give us the population of E at each ionization stage and excitation level (r, s). We found that the density, and hence the line strength, depends primarily on temperature. We use this to show that the reason the CaII K line is stronger than the Hα line in the stellar photosphere is due to CaII($s = 2$) is more abundant than HI($s = 1$) at these temperatures, and hence less sensitive to temperature change. To find the shape and origin of spectral lines, we use the reverse layer model, the Planck law, and we take into account the intensity produced by the gas itself along with the intensity that irradiates the gas. This showed that as the opaqueness τ increase, more and more of the initial incoming intensity is blocked. We call this an optically thick medium, as opposed to optically thin, where most of the intensity can pass unhindered through he gas. We find that the thermal motions of particles and their interactions with one another change the shape of the line profile from a Doppler profile to a Lorentzian profile with broad wings as the opaqueness τ increase. An optically thick medium produce stronger emission and absorption lines than a optically thin medium. The shape of the spectral line affect the curve of growth W_λ. A Doppler profile result in a linear curve, a Lorentzian in a linear curve but with a smaller slope, and the area between them has the shortest growth of all, representing when the line profile become saturated. We conclude that the opaqueness of the gas and the interactions and motions of atoms and ions that produce the spectral lines, affect the shape and strength of spectral lines.

1. Introduction

We follow in the footsteps of Cecilia Payne and Marcel Minneart to understand what determines the strength of solar spectral lines, and how these lines originate and what factors determine their shape. We do this by applying the Saha- and Boltzmann laws for matter, and the Planck law for radiation. The methods used are shown in the next section. The results and their analysis by using Payne's methods get one section each, Section 3 and 4, while for Minneart's method the results and their analysis are in one section Section 5. Lastly follows the conclusion and the appendix.

2. Method

Here we presents the methods used in part one and two of the exercise.

2.1. Schadeenium

To reproduce Schadee's three tables of the element Schadeenium (E), we use the Boltzmann distribution, its partition function, and the Saha distribution function, respectively defined as

$$\frac{n_{r,s}}{N_r} = \frac{g_{r,s}}{U_r} \mathrm{e}^{-\chi_{r,s}/kT} \tag{1}$$

$$U_r = \sum_s g_{r,s} \mathrm{e}^{-\chi_{r,s}/kT} \tag{2}$$

$$\frac{N_{r+1}}{N_r} = \frac{1}{N_e} \frac{2U_{r+1}}{U_r} \left(\frac{2\pi m_e kT}{h^2} \right)^{3/2} \mathrm{e}^{-\chi_r/kT}, \tag{3}$$

where $g_{r,s}$ is the statistical weight of ionization stage r and excitation level s, $\chi_{r,s}$ is the excitation energy of level s measured from the ground state $(r, 1)$, χ_r is the ionization energy measured from the ground state, k is the Boltzmann constant, T is the temperature, $n_{r,s}$ is the particle density at level (r, s) and are called level populations in units of cm^3. $N_r = \sum_s n_{r,s}$ is the total particle density for all ionization stages r, N_e is the electron density, m_e the electron mass, and h is the Planck constant.

The schadeenium element (E) in particular has ionization energies $\chi_1 = 7$ eV, $\chi_2 = 16$ eV, $\chi_3 = 31$ eV and $\chi_4 = 51$ eV. The excitation energies $\chi_{r,s}$ increase incrementally by 1 eV in each stage, so $\chi_{r,s} = s - 1$eV. The statistical weight is constantly equal to one for all levels, $g_{r,s} = 1$.

We evaluate equations 1-3 at the temperatures $T = 5\,000$ K, 10 000 K and 20 000 K, and check that our values are equal to those in Schadee's tables. We use an electron pressure of $P_e = 10^3$ dyne cm^{-2} to calculate the electron density by using the ideal gas equation

$$N_e = \frac{kT}{P_e}. \tag{4}$$

We assume, like Payne, that the strength of the spectral lines formed at level (r, s) scale with the lower level population $n_{r,s}$ as predicted by the Saha-Boltzmann distribution. This assumption is actually incorrect, which is discussed further in Section 4.

We get the Saha-Boltzmann distribution $n_{r,s}/N$ simply by multiplying Equation 1 with Equation 3 normalized with $N = \sum_r N_r$,

$$\frac{n_{r,s}}{N} = \frac{n_{r,s}}{N_r} \cdot \frac{N_r}{N}. \tag{5}$$

We plot this distribution and get Payne curves for stages $r = 1 - 4$ and levels $s = 1 - 4$ against temperature. We use the same electron pressure as Payne used, $P_e = 131$ dyne cm^{-2}.

2.2. Spectral line strength ratios

Like Cecilia Payne, we will work under the assumption that the spectral line strength scales with the population density of an excitation level s within an atom or ion. We use this to calculate the strength ratios between the different HI α lines in the Lyman (Ly), Balmer (Ba), Paschen (Pa), and Brackett (Br) series. This means the transitions $s = 2-1$, $s = 3-2$, $s = 4-3$, and $s = 5-4$ respectively. The general equation is

$$\frac{n_{1,s}}{n_{1,s+1}} = \frac{g_{1,s}e^{-\chi_{1,s}/kT}}{g_{1,s+1}e^{-\chi_{1,s+1}/kT}} \tag{6}$$

where for hydrogen the statisitcal weight is $g_{r,s} = 2s^2$. The excitation energies are $\chi_{1,s} = [0, 10.20, 12.09, 12.75]$ for $s = 1, ..., 4$.

2.3. Analysing the CaII K and Hα lines

When calculating the Saha-Boltzmann populations for the hydrogen atom and its ion, we follow the same procedures as for schadeenium. We still use equation 1-3, but we have a few different parameter values. For hydrogen, the statistical weight is $g_{r=1,s} = 2s^2$ for the ground state, and $g_{2,1} = 1$ for its only ion stage. The excitation energies are $\chi_{1,s} = 13.598(1 - 1/s^2)$ eV. The partition function has the value $U_2 = 1$.

For calcium, we have the ionization energies $\chi_r = [6.113, 11.871, 50.91, 67.15]$, but otherwise we use the same parameter values as for schadeenium. The abundance of Ca in the sun is $2 \cdot 10^{-6}$, where the abundance of hydrogen is 1.

We are interested in comparing the CaII K line strength with the Hα line strength. The $H\alpha$ line comes from the transition from $(1, s = 3)$ to $(1, s = 2)$, while the CaII K spectral line comes from the transition $(2, s = 2)$ to $(2, s = 1)$. As we assume the strength ratio of the line scales linearly with the population density at a level s, we calculate the CaII($s = 1$) population and the HI($s = 2$) population by using the Saha-Boltzmann distribution for $P_e = 10^{-2}$dyne cm^{-2} at the level $(r = 1, s = 2)$ for hydrogen, and level $(r = 2, s = 1)$ for calcium. To estimate the solar line strength ratio of CaII($s = 1$), we multiply its population with its solar abundance, and divide by the HI($s = 2$) population. We plot this ratio against temperature.

To analyze the temperature sensitivity of the two lines, we calculate the relative population change. We find the slope of the population by computing the difference in population density at the temperature T and at $T + \Delta T$ and dividing by ΔT, and we get the relative change by dividing with $n_{r,s}$,

$$\left|\frac{\Delta n_{CaII(s=1)}}{n_{CaII(s=1)}\Delta T}\right| = \left|\frac{n_{CaII(s=1)}(T) - n_{CaII(s=1)}(T + \Delta T)}{n_{CaII(s=1)}\Delta T}\right| \tag{7}$$

$$\left|\frac{\Delta n_{HI(s=2)}}{n_{HI(s=2)}\Delta T}\right| = \left|\frac{n_{HI(s=2)}(T) - n_{HI(s=2)}(T + \Delta T)}{n_{HI(s=2)}\Delta T}\right|. \tag{8}$$

In our case, we have put $\Delta T = 1$K

Lastly in part one of this exercise, we wish to find the fraction of neutral hydrogen as a function of temperature. To do this, we compute the Saha-Boltzmann function for hydrogen at $r = 1$, and plot the results against temperature.

2.4. Formation of spectral lines

In part two of this exercise, we will examine how spectral lines form. The Planck function specifies the radiation intensity emitted by a gas or black body in thermal equilibrium (TE). It is defined as

$$B_\lambda(T) = \frac{2hc^2}{\lambda^5}\frac{1}{e^{hc/\lambda kT} - 1}, \tag{9}$$

where c is the speed of light, λ is the wavelength in units of Ångström(Å) and the other constants are previously defined. The function has the units erg cm^{-2}s^{-1}steradian^{-1}. We plot this function for various temperatures T against λ to see how the intensity vary with temperature and wavelength.

To measure the total amount radiation intensity that is emitted from a gas, which takes into account absorption of incoming radiation intensity and the radiation produced by the gas itself, we have the expression

$$I_\lambda = I_\lambda(0)e^{-\tau} + \int_0^\tau B_\lambda[T(x)]e^{-(\tau-\tau(x))}\mathrm{d}\tau(x), \tag{10}$$

where I_λ is the total intensity emitted from a gas with the same units as the Planck function, τ is the optical thickness at the boundary of the gas, $\tau(x)$ is the optical thickness at the position x within the gas, and $T(x)$ is the temperature at position x. The first term on the right-hand-side is the weakened intensity that emerges on the other side of the gas that comes from the original incoming intensity $I_\lambda(0)$. The second term is the intensity produced by the gas itself. For an isothermal layer where $B_\lambda[T(x)]$ does not depend on x, we can calculate the integral in Equation 10

$$\begin{aligned}\int_0^\tau B_\lambda[T(x)]e^{-(\tau-\tau(x))}\mathrm{d}\tau(x) &= B_\lambda(T)e^{-\tau}\int_0^\tau e^{\tau(x)}\mathrm{d}\tau(x)\\ &= B_\lambda(T)e^{-\tau}[e^\tau - 1]\\ &= B_\lambda(T)[1 - e^{-\tau}],\end{aligned}$$

and the final expression for the emergent intensity is then

$$I_\lambda = I_\lambda(0)e^{-\tau} + B_\lambda(T)[1 - e^{-\tau}] \tag{11}$$

We plot this equation against τ for $B_\lambda = 2$ erg cm^{-2}s^{-1}steradian^{-1} and for several initial incoming intensity values $I_\lambda(0) = [0, 1, 2, 3, 4]$ erg cm^{-2}s^{-1}steradian^{-1}.

To find the spectral lines intensity profile we use the Schuster-Schwarzchild or reversing-layer model. This model assumes that continuous radiation is emitted at the steller surface, which has the temperature $T_{surface}$, with the intensity $I_\lambda(0) =$

$B_\lambda(T_{surface})$. This intensity irradiates a layer surrounding the surface with temperature T_{layer}, and that consists only of atoms and ions that cause spectral lines.

A spectral line is not sharply defined at one wavelength, but is slightly "spread out". This line broadening is described by

$$\tau(u) = \tau(0)V(a,u), \tag{12}$$

where V is the Voigt function, $u = \Delta\lambda/\Delta\lambda_D$ is the dimensionless wavelength separation $\Delta\lambda = \lambda - \lambda(0)$ from the center of the spectral line at $\lambda = \lambda(0)$, $\Delta\lambda_D$ is the Doppler width, $\tau(0)$ is the optical depth at the wavelength at the center of the spectral line, and a is called dampening and is a measure of the amount of Coulomb disturbances. An approximation to the Voigt function is defined as

$$V(a,u) \approx \frac{1}{\Delta\lambda_D\sqrt{\pi}}\left[e^{-u^2} + \frac{a}{\sqrt{\pi}u^2}\right]. \tag{13}$$

We do not numerically implement this function ourselves, but call on one that already exists in the `scipy` library. We plot the Voigt profile against u for several $a = [0.001, 0.01, 0.1, 1.0]$.

The stellar spectral line profiles are found by combining Equation 11 with Equation 13. We do this by using Equation 12 to calculate τ. We plot the line profiles, that is, the intensity I_λ against u, for $\log_{10}\tau(0) = -2$ to 2 , and a temperature for the surface of the gas $T_{surface} = 5\,700$ K and a layer temperature $T_{layer} = 4\,200$. We do this for the wavelengths $\lambda = 2\,000,\ 5\,000,\ 10\,000$ Å.

To show the relative intensity, we plot $I_\lambda/I_\lambda(0)$ for $\tau(0) = [0.01, 1, 50]$ against u for the same wavelengths.

The equivalent width W_λ is a line-strength parameter. It is a measure of the growth of the absorption feature of spectral line profiles, and is defined as

$$W_\lambda = \int \frac{I_{cont} - I(\lambda)}{I_{cont}}\mathrm{d}\lambda. \tag{14}$$

where I_{cont} is the intensity of the continuum. So it is a rectangular block of the same area as the area under the line profile. We plot the equivalent width for several τ to get a curve of growth. The curve of growth shows the dependence on the growth of the line strength with the density of the material where the line is created.

3. Results part 1

Here we show the results we got from implementing our methods in Section 2 for the first part of the exercise. Only the results are presented here, they will be analyzed and discussed in Section 5.

3.1. α lines strength ratios

The population density ratio between the Lyman, Balmer, Paschen and Brackett at the lower level of the α line transition in each series, is shown in Table 1 at different temperatures T. We see that as the temperatures increase, the ratios become smaller.

3.2. Schadee's table and Payne curves for schedeenium

When evaluating the Saha and Boltzmann distributions and their partition function as described in equations 1-3 for element E, at different temperatures T, we get the results in Table 2. We see that our values coincide with the values calculated by Schadee. The partition function seems to barely be sensitive to temperature and ionization stage, every value being of order unity.

In the Boltzmann distribution table, we have steep population decay, but it is less steep for higher temperatures. We note that while the ground state population decrease as the temperature increase, it is never depleted and always have the greatest value of all the excitation levels.

In the Saha distribution table, there are only two ionization stages with a significant particle density at a time, at each temperature. At T=5 000 K, neutral Schadeeium (EI) has the greatest density with $N_1/N = 0.906$, and E ionized once (EII) have the second largest with $N_2/N = 0.0939$. For T=10 000 K, the ions EII and EIII have the greatest density, the third greatest density belongs to the ground state, it being on the scale of 10^{-4}. For T = 20 000 K, EIII and EIV have the greatest particle density, while the third largest is again on the scale of 10^{-4}.

Table 1: α line ratios

Line ratio	$T = 5\,000$ K	$T = 10\,000$ K	$T = 20\,000$ K
Ly α/Ba α	$4.78{\cdot}10^9$	$3.45 \cdot 10^4$	92.94
Ba α/Pa α	40.17	4.48	1.50
Ba α/Br α	92.94	4.82	1.10
Pa α/Br α	2.31	1.08	0.73

The population density ratio between the Lyman, Balmer, Paschen and Brackett at the lower level of the α line transition in each series at the temperatures $T = 5\,000$, 10 000, 20 000 K.

Table 2: Saha-, Boltzmann distribution and partition function

U_r	$T = 5\,000$K	$T = 10\,000$ K	$T = 20\,000$ K
U_1	1.109	1.456	2.232
$U_2 = U_3 = U_4$	1.109	1.456	2.271
$n_{r,s}/N_r$	$T = 5\,000$K	$T = 10\,000$ K	$T = 20\,000$ K
$s = 1$	0.902	0.687	0.448
2	0.0885	0.215	0.251
3	$8.694 \cdot 10^{-3}$	0.0674	0.140
4	$8.536 \cdot 10^{-4}$	0.0211	0.0786
5	$8.381 \cdot 10^{-5}$	$6.623 \cdot 10^{-3}$	0.0440
6	$8.229 \cdot 10^{-6}$	$2.075 \cdot 10^{-3}$	0.0246
7	$8.080 \cdot 10^{-7}$	$6.501 \cdot 10^{-4}$	0.0138
10	$7.648 \cdot 10^{-10}$	$2.000 \cdot 10^{-5}$	$2.417 \cdot 10^{-3}$
15	$6.978 \cdot 10^{-15}$	$6.042 \cdot 10^{-8}$	$1.329 \cdot 10^{-4}$
N_r/N	$T = 5\,000$K	$T = 10\,000$ K	$T = 20\,000$ K
$r = 1$	0.906	$4.784 \cdot 10^{-4}$	$2.735 \cdot 10^{-10}$
2	0.0938	0.9452	$1.806 \cdot 10^{-4}$
3	$8.242 \cdot 10^{-12}$	0.0543	0.632
4	$5.499 \cdot 10^{-37}$	$8.620 \cdot 10^{-11}$	0.368
5	$4.588 \cdot 10^{-82}$	$1.562 \cdot 10^{-29}$	$1.716 \cdot 10^{-6}$

All three tables are evaluated at the temperatures T=5 000 K, 10 000 K and 20 000 K. The first table shows the partition function evaluated at different r as specified in the table. The second table shows the Boltzmann distribution at different excitation levels s for $r = 1$. The third table shows the Saha distribution at different ionization stages r, divided by $N = \sum_r N_r$.

The Saha-Boltzmann population distribution of element E is plotted against temperature in Figure 1. The y-axis is scaled with $\log_{10}$. We see that the curves consist of tops with steep slopes on either side. The level $(r = 1, s = 1)$ has the highest population of all the possible (r, s) pairs. This is neutral schadeenium in its ground state. When the atom or ion is excited, it is ion EIV that has the largest population for all $s > 1$, then follows EIII, EII, and EI, neutral schadeenium having the smallest population of them all. However for every stage r, the ground state always have the highest population, also compared to other excitation levels $s > 1$ of other stages r. The population gap between the ground state and the first excited level and between excited levels, decrease as E become more ionized.

We also see that the curves overlap, and that level $(r = r + 1, s)$ for any s, start increasing before level (r, s) has started depleting. In general, as the (r, s) curves decrease, the $(r + 1, s)$ curves increase rapidly. Simply by eyeing the curves, and the values in Table 2, we see that the curves correspond to multiplying the second and third part of the table, which is what we expect.

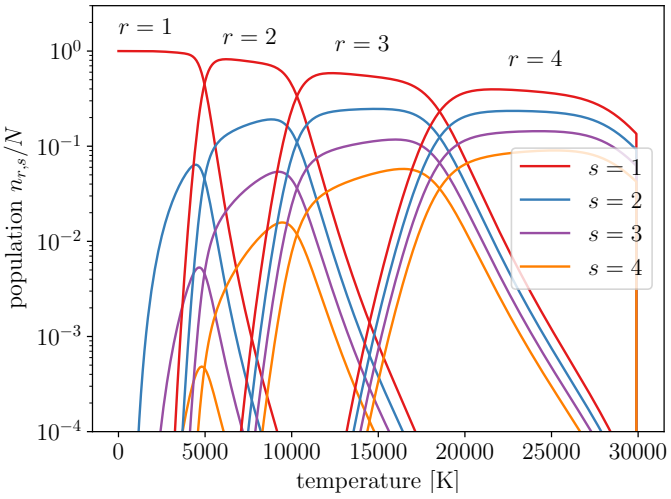

Fig. 1: The Saha-Boltzmann distribution for various ionization stages r and excitation levels s for element schadeenium E. The y-axis is shown in a $\log_{10}$ scale

3.3. Ca II K vs Hα: line strength and temperature sensitivity

The population ratio between Ca II($s = 1$) and the HI($s = 2$) is shown in Figure 2. We see that at the temperatures of the solar photosphere, $T = 4\,000 - 6\,000$ K, the CaII($s = 1$) population is larger than that of HI($s = 2$). At $T = 5\,000$ K the ratio CaII($s = 1$)/H($s = 2$) is 7642.56.

The relative population change $(\Delta n_{Ca}/\Delta T)/n_{Ca}$ and $(\Delta n_H/\Delta T)/n_H$ for a small change in temperature $\Delta T = 1$ K is shown in Figure 3 as a function of temperature. The relative population of each element is over-plotted with dashed lines. We see that a dip in the population change correspond to a flat peak in the population of the same element. This happens for Calcium at T =5 600 K, and for Hydrogen at $T = 9\,500$ K. We notice the steep slopes of the relative population density on either side of the peak, indicating a rapid increase or decrease in the population at these temperatures. On the curves of the relative popula-

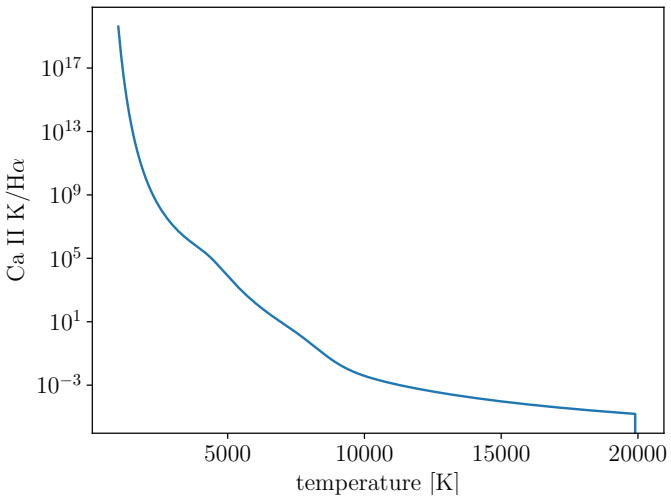

Fig. 2: The population ratio of Ca II($s = 1$) ion and the HI($s = 2$) atom in the sun, and thereby the strength ratio between the CaII K line and the Hα. It shows that in the solar photosphere (T= 4 000-6 000 K), the CaII K line is dominant, and stronger than the Hα line. The y-axis is scaled with $\log_{10}$.

tion change, the left flank has a negative slope, so $\Delta n < 0$, while the right flank has a positive slope, meaning $\Delta n < 0$.

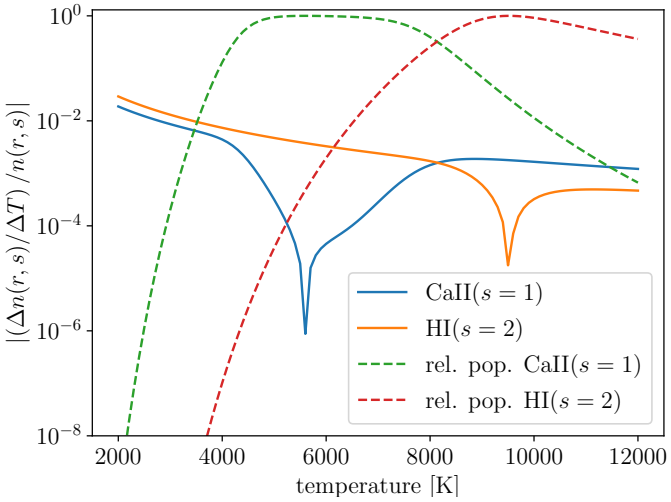

Fig. 3: Relative population change as a function of temperature is shown with whole lines for CaII K and Hα. The relative population of the elements are over-plotted with dashed lines. We see that a valley in the population change correspond to a peak in the population of the same element. The y-axis is scaled with $\log_{10}$.

3.4. Neutral hydrogen fraction in stars

In figure 4 the fraction of neutral hydrogen in stellar photospheres at different temperatures are shown. The point where 50 % of the neutral hydrogen is ionized is marked with and orange dot. This happens approximately at a temperature of $T = 9\,216$ K. This marks the transition between "cold" stars and "hot" stars.

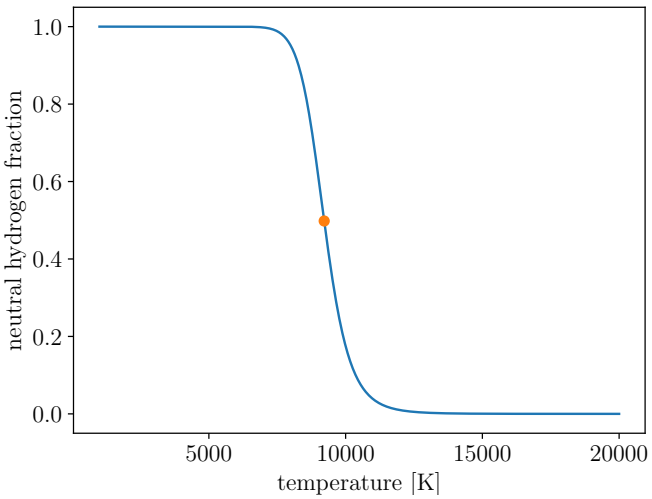

Fig. 4: Ratio of neutral hydrogen for different temperatures. The temperature at which 50 % of the neutral hydrogen has been ionized, is marked with an orange dot, occurring at $T = 9\,216$ K.

4. Analysis part 1

Payne's basic assumption that the spectral line strength scales with the lower level population density, is incorrect. While it is true that the lowest levels have the largest population density, the line strength scale with the excitation energy. The energy gap between the ground state and the first excited level is in most elements the largest one, with the energy needed to excite the atom further, decreasing between the levels as s increase. This results in the transition $s = 2 - 1$ producing a stronger spectral line than $s = 3 - 2$. For the hydrogen atom, the spectral line strength is proportional to the inverse of the energies of the lower level, $1/E = -n^2/(13.6\,\mathrm{eV}) \propto n^2$ where $n = s$ is the principal quantum number, which is a second order polynomial. It does not scale linearly with the population density like Payne assumed, and as we showed in Table 2.

From part 2 of Table 2 we see that as the temperature increase, the atoms become excited, although excitation never fully depletes the ground state. From looking at Equation 1, the Boltzmann factor becomes smaller for lower s, which is why the ground state is never depleted and the lower levels have the highest population, regardless of temperature. As T increase, the Boltzmann factor become even smaller, resulting in less steep decay, and gives larger population density to higher s. The partition function $U_{r,s}$ grows slightly with temperature, but it maintains the order of unity, however this does make the population decay slightly larger in the Boltzmann distribution.

The third part of the table shows that as T increase, only certain ionization stages have any noteworthy particle density. The Saha distribution also have a Boltzmann factor that increase as r is low and T is large, the expression also contain a $T^{3/2}$ factor. The reason why the lower stages r can be depleted as T increase, unlike in the Boltzmann distribution, comes from the fact that the particle density at stage r, N_r, is proportional to the particle density at the previous stage $r - 1$, $N_r \propto N_{r-1}$. So if N_r is large, the next level density, N_{r+1} become even larger in the cases where the Boltzmann factor does not dominate, which it does for high r and low T. This is why we only have two significant ionization stages at each temperature, because for r higher than these stages, the Boltzmann factor dominates, making the particle density small.

The curves in Figure 1 all have steep slopes on either side of their peaks. Their steepnes comes from the fact that as the temperature increase, element E receive enough energy to become either excited or ionized, or both, and so as the population of $(r = 1, s = 1)$ decrease, the population of the next ionization stage become larger, though never as large as the ground state of neutral E. This is only true for the ground state of each atom-/ion. For the first excitation level $s = 2$, it is ion EIV that has the largest population.

In general the population gap between the ground state and excited levels decrease the higher the ionization stage. This is due to the fact that as the temperature increase, atoms and ions receive more energy, as there are more collisions. They become increasingly easy to ionize and ionize further, and also easier excited for the same reasons. So the population difference between the levels s is smaller for higher degrees of ionization.

We see that the curve of level $(r = r+1, s)$ for any s, start increasing before level (r, s) has started depleting. This is because particles from the excited states are sometimes ionized first like $(r, s + 1)$, as the ionization energy from an excited state is less than from the ground state. In general, as the (r, s) curves decrease, the $(r+1, s)$ curves increase rapidly, as the particles move from one level to another.

From Figure 2, we have that at the temperatures of the solar photosphere, $T = 4\,000 - 6\,000$ K, the CaII$(s = 1)$ population is larger than that of HI$(s = 2)$. As the line strength of spectral lines scale with the lower level population density, the CaII K line is stronger than the Hα line in this region.

In Figure 3, there is a dip in the curves of the relative population change. This means that at $T = 5600$ K the HI$(s = 2)$ is more sensitive to temperature change than CaII$(s = 1)$ is. We also see this from the relative population of each element. When the change in population is at a minimum, the relative population curve is close to constant, meaning that in this temperature range, a change in temperature does not affect the population density. This is due to the fact that at this temperature, most calcium atoms have been ionized to CaII, and so the population of CaII$(s = 1)$ is high, meaning the temperature would have to increase further and ionize or excite much of the CaII$(s = 1)$ ions to make the population density decrease. The the ground state $s = 1$ population is as stated quite abundant compared to he HI$(s = 2)$ at this temperature. At other temperatures we see the steep slopes of the relative population curves, meaning that at these temperatures, the population increase or decrease rapidly, and is quite temperature sensitive, which we can also see by the small slope in the population change curves.

5. Results and analysis part 2

Here we present the results for the second part of the exercise, regarding the formation of spectral lines. The results are also commented and analyzed here.

5.1. Planck curves

When we evaluate the Planck function given by Equation 9 for a temperature of $T = 5\,000$ K and a wavelength of $\lambda = 5\,000$ Å, we get that its value is $1.207 \cdot 10^{14}$ erg cm^{-2}s^{-1}steradian^{-1}. Planck

curves for various temperatures and wavelengths are shown in Figure 5.

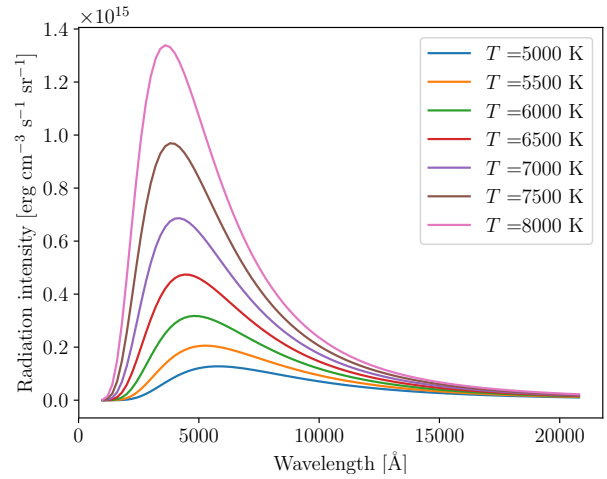

a)

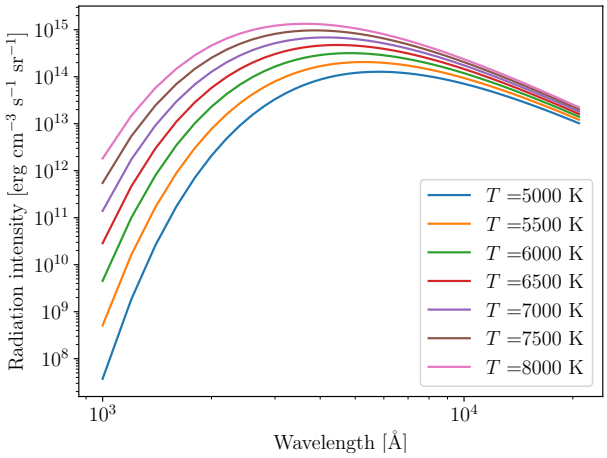

b)

Fig. 5: The Planck function evaluated at different temperatures T. The second figure shows the same thing but with logarithmically scaled axes. From the second plot we see that for wavelengths larger than $\lambda \sim 10^4$, the radiation intensity become less dependent on temperature, all the different curves converging closer together. At short wavelengths, up to around $\lambda = 5\,000$ Å, the intensity increase exponentially with the wavelength. From the first plot we see that the maximum radiation intensity is emitted around the wavelength $\lambda = 5\,000$ Å regardless of temperature. Both plots show that the higher the temperature, the higher the intensity. The curve of $T = 8\,000$ K has the largest value at every wavelength, the = 7 000 K curve has the second largest intensity at every wavelength, and so forth down to the curve with the lowest intensity at $T = 5\,000$ K.

5.2. Radiation through isothermal layer

The emergent intensity I_λ specified in Equation 11 is plotted against the optical thickness τ in Figure 6. In the second plot the y-axis is logarithmic.

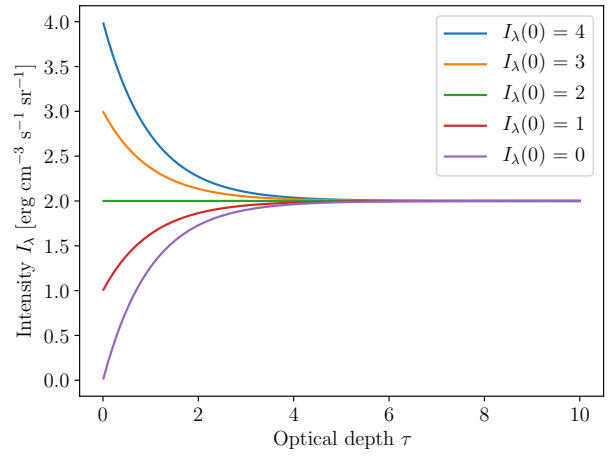

a)

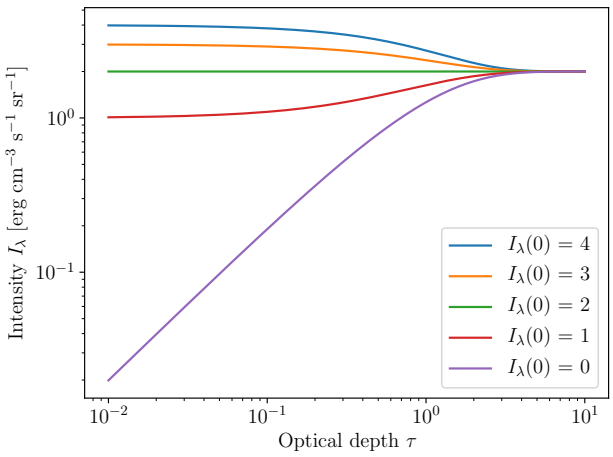

b)

Fig. 6: The emergent intensity from a gas cloud for several initial intensities $I_\lambda(0)$ is shown. The second plot has a logarithmic x- and y-axis For $\tau \ll 1$ and $I_\lambda(0) = 0$, we can see from the second plot that I_λ depend linearly on τ. When $\tau \ll 1$ and $I_\lambda(0) > B_\lambda$, $I_\lambda(0)$ is constant, regardless of τ. A layer at a $\tau \ll 1$ is called optically thin, because much, if not all of the incoming radiation intensity, escapes unhindered through the media. We see that for $\tau \gg 1$, the emergent intensity is equal to $B_\lambda = 2$ erg cm^{-2}s^{-1}steradian^{-1}, regardless of the initial intensity. B_λ is the radiation produced by the gas itself, meaning that nothing of the incoming intensity $I_\lambda(0)$ has made it this deep into the gas. Which is why a medium with $\tau \gg 1$ is called optically thick, because no intensity radiation can pass beyond this point, all radiation emitted from beyond this layer can only have been produced by the medium itself. A reason for this can be that the material is very dense.

5.3. Spectral lines from solar reversing layer

The Voigt profile for the a values specified in the method section, is shown in Figure 7. The y-axis is logarithmically scaled. The plot with linear axes can be seen in the Appendix section. We see that for low a, the Voigt profile look more gaussian than Lorentzian, the wings of the profile beeing small. As a increase, the profile look increasingly Lorentzian, gaining bigger wings.

The Schuster-Schwarzschild line profiles can be seen in Figure 8. We see that at line center $u = 0$, the gas can be consid-

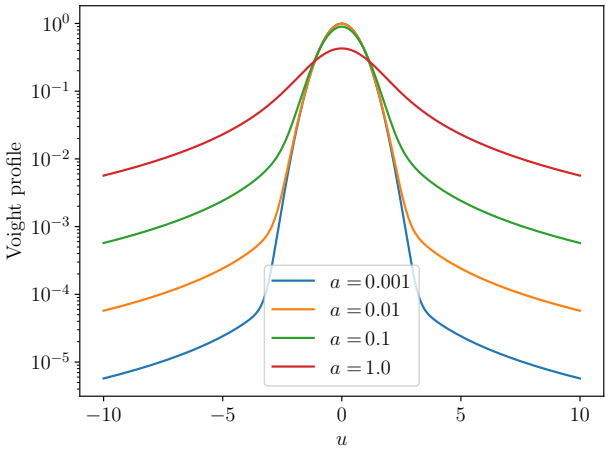

Fig. 7: Voigt profile against u, the y-axis is scaled logarithmically. We see that the larger a is, the broader is the wings on either side of the peak, and the peak has a lower height. The wings diminish as u increase. We see from the Voigt function in Equation 13, that a large u makes the profile smaller, while a big a will make it larger. A small damping parameter a results in a sharper, taller peak.

ered optically thick for $\tau(0) = 10$ and 50 for all wavelengths. At $u = 5$, only at $\tau = 50$, can the gas be considered optically thick.

The optically thin lines have broadening due to the random thermal motions of the particles where the line originates. This is called Thermal Doppler broadening, as the photons will be blue or red shifted by the Doppler effect, depending on their velocity relative to the observer. The lines have a Doppler profile, which is Gaussian shaped

For $\tau(0) \gg 1$, there is a low intensity saturation limit for all the wavelengths, and it becomes more pronounced as the wavelength increase. The intensity at the saturation limit is equal to that of $B_\lambda(T_{layer})$, and we can see from Figure 6 also, that a radiation intensity with a initial intensity $I_\lambda(0) < B_\lambda(T_{layer})$ can not decrease beneath this value, and as the optical thickness increase, the intensity of the spectral line will converge on this value. The value of this saturation limit depend on both the temperature of the layer the spectral lines come from, but also on the wavelength. The surface temperature and the wavelength decide the maximum intensity, I_{cont}

We see that line wings develop for big $\tau(0)$. This is called Pressure broadening, or Collisional broadening, as a denser material will lead to more collisions and interactions between particles, which will affect the radiation emitted. Pressure broadening become more dominant than Doppler broadening at high optical thickness. The absorption lines are strong for high optical thickness, and weak for low $\tau(0)$. The lines have a Lorentzian profile with long wings.

In Figure 9, the line profiles are shown with relative intensity on the y-axis. The optical density is here $\tau(0) = [0.1, 1, 50]$. Here we see that the relative intensity is the highest for $\lambda = 10\,000$ Å, and the lowest for $\lambda = 2\,000$ Å. The relative intensity increase with increasing wavelength.

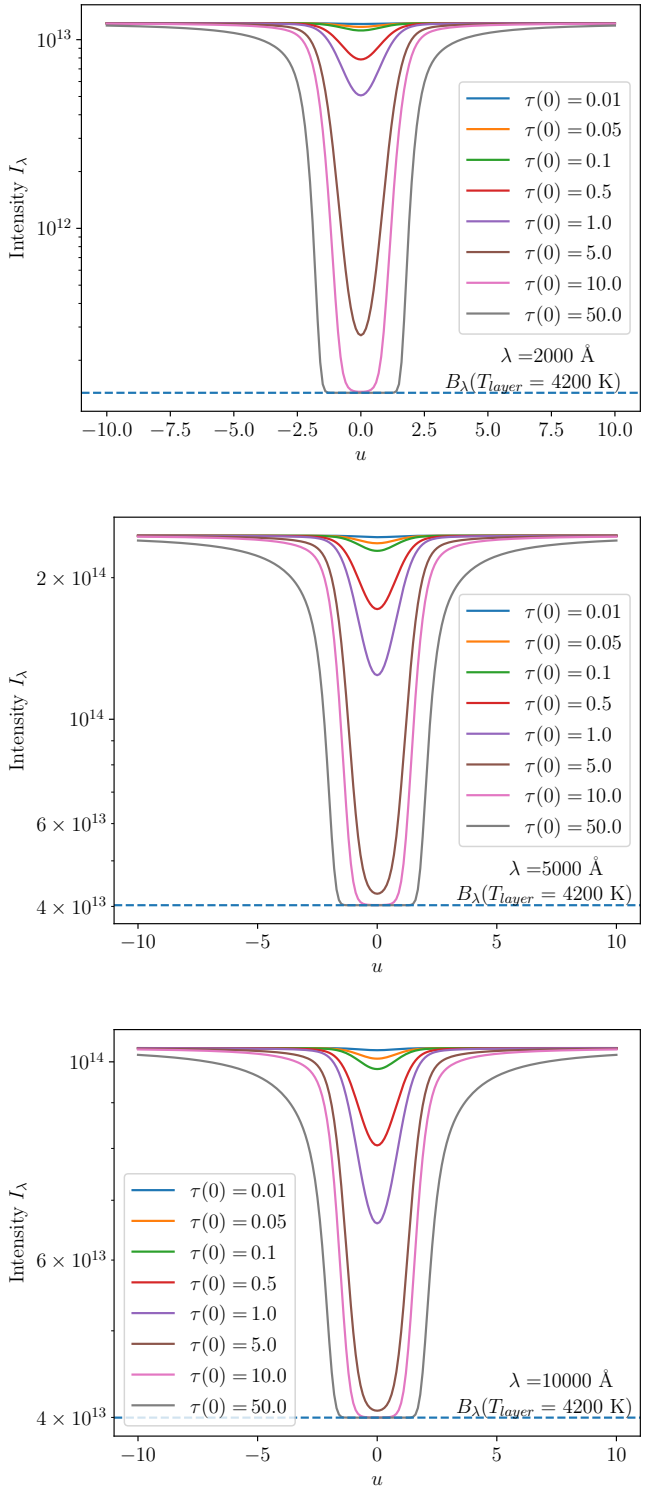

Fig. 8: The Schuster-Schwarzschild line profiles for different optical thicknesses $\tau(0)$ and the wavelengths $\lambda = 2\,000$, $5\,000$, $10\,000$ Å. We see that the absorption lines have the overall highest I_{cont} value at $\lambda = 5\,000$ Å. We see that the absorption lines are the strongest for high optical thickness, and weak for low $\tau(0)$

5.4. The curve of growth

At low $\tau \ll 1$, the spectral lines are characterized by a Doppler profile, which is Gaussian shaped. The thermal motions of the

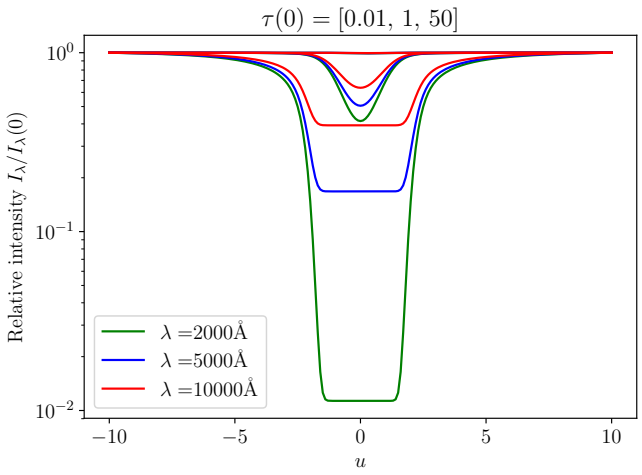

Fig. 9: The Schuster-Schwarzschild line profiles for different optical thicknesses $\tau(0)$ and the wavelengths λ = 2 000, 5 000, 10 000 Å with relative intensity on the y-axis, which is logarithmically scaled. We see that the relative intensity of the absorption lines increase with increasing wavelength.

particles cause the broadening. This correspond to the first linear part of the curve of growth in Figure 10. In part two the intensity of the absorption line becomes saturated, and the profile become more square, but the equivalent width increase very little, so this part in the curve of growth is flat. In part three, the lines are strong, as τ is large. The lines are now characterized by a Lorentzian profile, which has long wings which makes the equivalent width increase faster than in part 2, but not as much as in part 1.

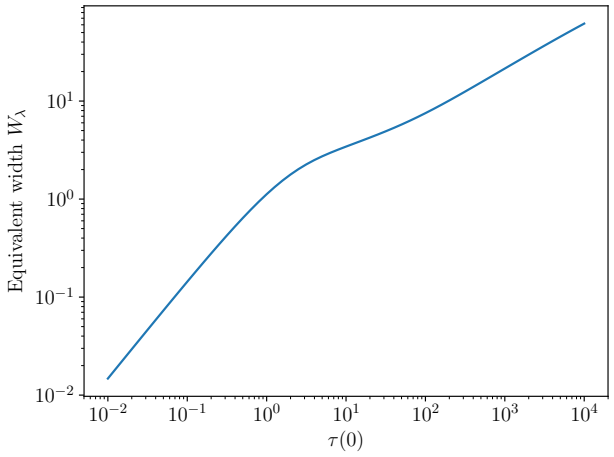

Fig. 10: The curve of growth shows the equivalent width W_λ as a function of the optical thickness τ.The area under the line profile grows rapidly for low τ as can be seen in Figure8, so the slope is 1:1 here. After the intensity reaches the saturation limit and the wings start too develop, the area start increasing again, but this time at a slower rate than for the Gaussian profiles, so the slope is 1:2 here. The damping parameter decides the onset of the third part. A high a result in a shorter midsection, meaning part three starts earlier.

To get emission lines instead of absorption lines, we would need to make the layer temperature T_{layer} higher than the surface temperature $T_{surface}$. For λ = 5 000 Å and T_{layer} =6 000 K where the other parameters remain the same as for the absorption line profiles, we get the emission line profiles and curve of growth in Figure 11.

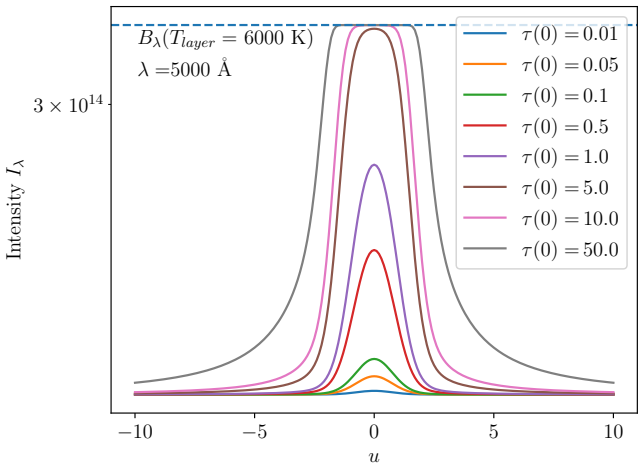

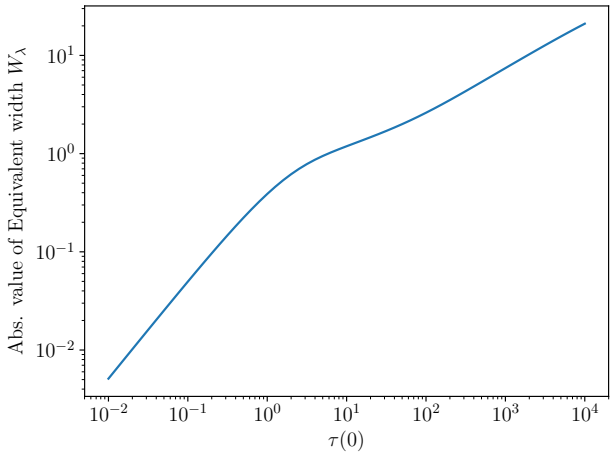

Fig. 11: Emission line intensity profile for various $\tau(0)$ and λ = 5 000 Å is shown in the first plot, and the curve of growth for emission lines in the next. The emission lines also get saturated at $B_\lambda(T_{layer})$ for high optical thickness $\tau(0)$. We see that the curve of growth looks the same for emission and absorption lines.

6. Conclusions

Cecilia Payne's assumption that the spectral line strength scales linearly with the lower level population density is incorrect. It scales with the inverse of the excitation energy between excitation levels s, which for hydrogen is proportional to s^2.

Working with Payne's assumption, we were able to reproduce Schadee's tables for the element schadeenium. We found that for the Boltzmann distribution, the Boltzmann factor cause exponential decay in population density per excitation level s, but that a high temperature T = 10 000 K result in less steep decay. The lower levels s have the largest population density.

The Saha distribution only have a significant particle density at two ionization stages r at a time for the temperatures T = 5 000, 10 000, 20 000 K. As T increase, the lower stages

are almost completely depleted. This is because the density at each stage depend on the density in the stage before, so if stage r has moderate high density, $r+1$ and $r+2$ will have even larger density until the Boltzmann factor become dominant, and there is steep exponential decay. The variations in the strength of the stellar spectral lines was found to be primarily due to temperature change.

We found that the reason for the steep curves on either side of the peaks in the Saha-Boltzmann distribution plot against temperature, was because an increase in temperature will reduce the population at a (r, s) as particles are excited to higher s levels, or ionized to higher r stages. The population density was shown to be quite sensitive to temperature change outside of the peak region. An increased temperature in the gas lead to more energy to the atoms/ions, which makes them ionize or excite at large numbers. For this same reason does the population gap between the ground state the excited levels, and between the excited levels themselves, become smaller at high temperatures.

The reason that the CaII K line is stronger than the Hα line was because in the temperature region $T = 4\,000\text{K} - 6\,000$ K, the solar photosphere, the level CaII($s = 1$) had a higher population density than the HI($s = 2$) level. At the temperature $T = 5\,600$ K the HI($s = 2$) population density is more sensitive to temperature change than the CaII($s = 1$) population. This is due to the fact that at this temperature, most calcium atoms have been ionized to CaII, and so the population of CaII($s = 1$) is high, meaning the temperature would have to increase further and ionize or excite much of the CaII($s = 1$) ions to make the population density decrease. The the ground state $s = 1$ population is quite abundant compared to he HI($s = 2$) at this temperature. At $T = 9\,500$ K, it is HI($s = 2$) that is the least sensitive to temperature.

When evaluating the Planck function, we found that for $\lambda > 5\,000$ Å, the radiation intensity became less dependent on temperature. Up until this point, the intensity had increased exponentially with wavelength, reaching a peak around $\lambda = 5\,000$ Å

For radiation trough an isothermal layer, we saw that for $\tau \ll 1$, which we call an optically thin layer, and incoming intensity $I_\lambda(0) = 0$ erg cm^{-3}s^{-1}sr^{-1}, the intensity is linearly proportional to τ. As τ increased, the radiation intensity became independent of $I_\lambda(0)$, and reach the value B_λ, meaning that the medium is optically thick and all of the initial incoming radiation had been blocked at this τ.

Using the solar reversing model we found that a high τ produce the strongest emission and absorption lines. For small τ, the spectral line profile looks Gaussian. The broadening is due to the thermal movements of the line-causing particles. For moderately high τ, the line profile become more square and saturated, while for high τ, the spectral lines get a Lorentzian profile with long wings due to pressure broadening. A big dampening parameter makes the profile look Lorentzian as opposed to Gaussian, as was seen in the plotting of the Voigt profile plot. We also found that the relative strength of the absorption lines decrease as wavelength increase.

We found that the curve of growth depend on the opaqueness of the material. The Doppler line profile produce a linear curve of growth, the Lorentzian profile gives a linear curve of growth with slope 1:2. The area in between them represent the transition between the two, when the profile become saturated, and the equivalent with increase slowly. A large damping parameter a will result in the third part of the growth occurring sooner.

In this exercise, we have found that the spectral line strength depend highly on temperature and that the shape of the spectral lines and their intensity depend on the opaqueness of the material, and on the interactions and motions of the atoms and ions where the spectral lines originate.

Acknowledgements. We are much indebted to Rob Rutten for exemplary instruction. We made much use of NASA's Astrophysics Data System.

7. Appendix

Here we show some additional plots. The Planck curve with only logarithmic y-axis is shown in Figure 12

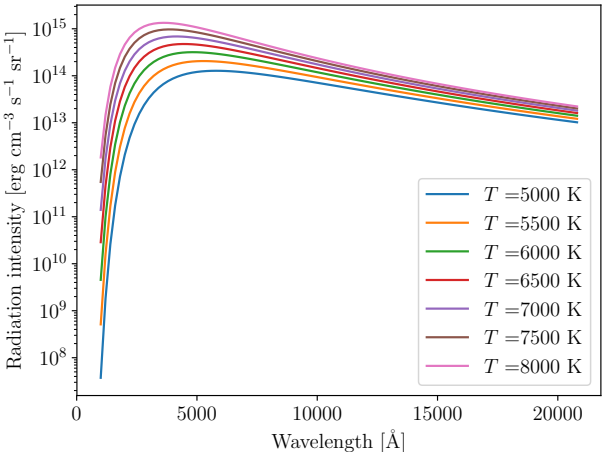

Fig. 12: The Planck function evaluated at different temperatures T. We see that for wavelengths $\lambda < 5\,000$ Å, the intensity increase rapidly, and for $\lambda > 5\,000$ Å it decreases at a slower rate.

The Voigt profile with linear axes is shown in Figure 13

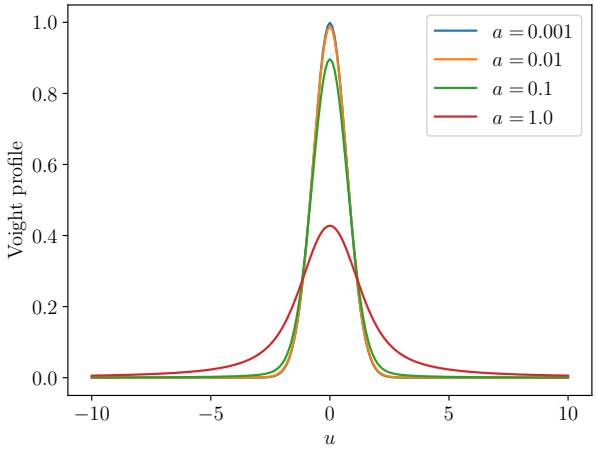

Fig. 13: The plot shows that a high damping factor a, makes the peak shorter and the wings of the profile broader. We see that the Voigt profile is a convolution of a Gaussian and a Lorentzian profile. As a increase, the profile become more Lorentzian looking.